Cell Reports Medicine, Volume *2*

Supplemental information

A muscle fatigue-like contractile decline was recapitulated using skeletal myotubes from Duchenne muscular dystrophy patient-derived iPSCs

Tomoya Uchimura, Toshifumi Asano, Takao Nakata, Akitsu Hotta, and Hidetoshi Sakurai

Supplementary information

Figure S1

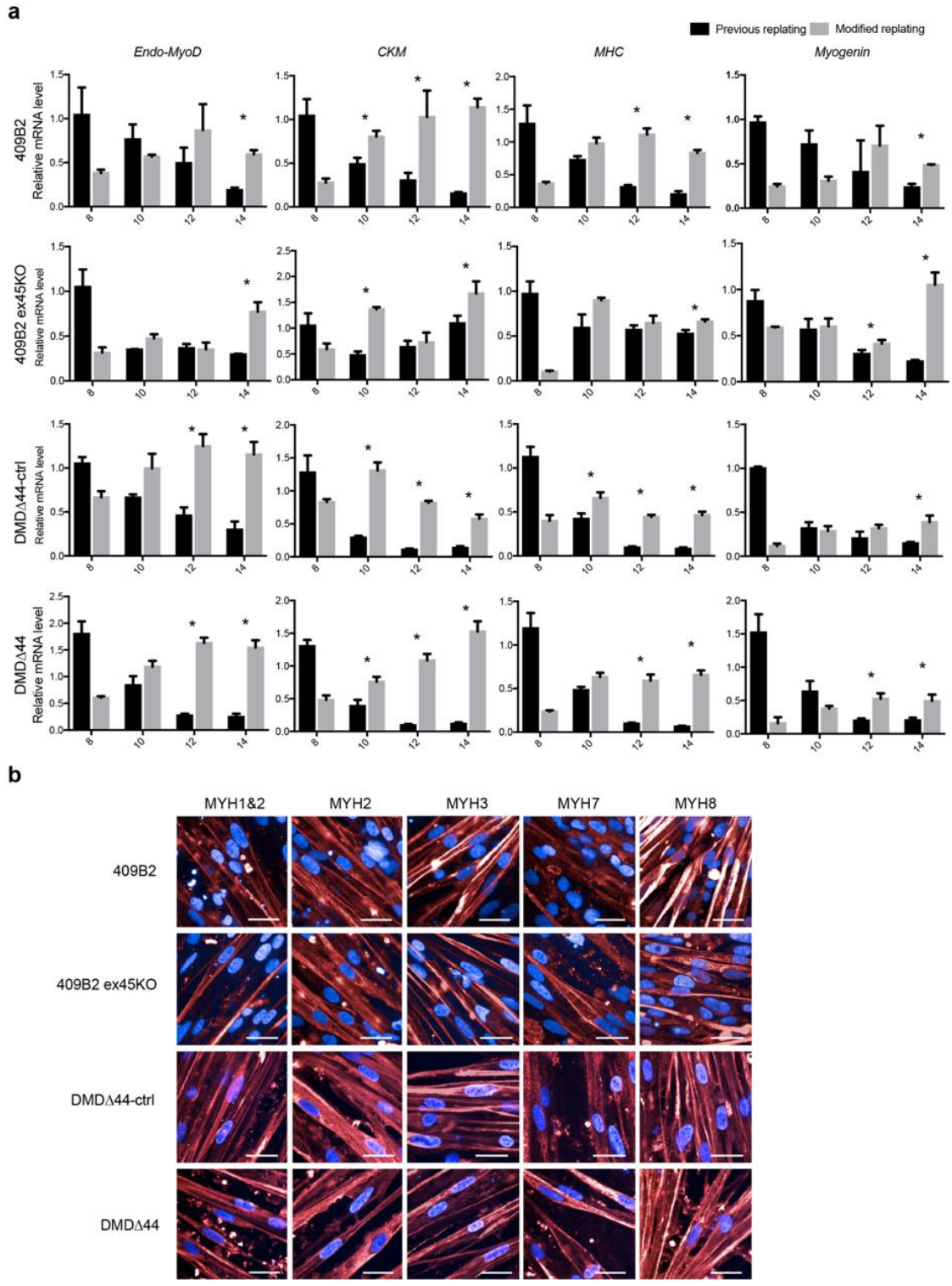

Figure S1. Gene expression analyses of hiPSC-skeletal myotubes differentiated by the modified replating method. (A) RT-qPCR analysis of endogenous-MyoD, CKM, MHC, and myogenin of 409B2, 409B2 ex45KO, DMDΔ44-ctrl, and DMDΔ44 myotubes differentiated by previously described and modified replating methods. Data represent the mean ± SD and were analyzed with an unpaired *t*-test from three biological replicates. * indicates $P < 0.05$ (B) Immunocytochemical analysis of each type of MYH of 409B2, 409B2 ex45KO, DMDΔ44-ctrl, and DMDΔ44 myotubes differentiated by previously described and modified replating methods. Scale bar = 20 μm. Related to Figure 1.

Figure S2

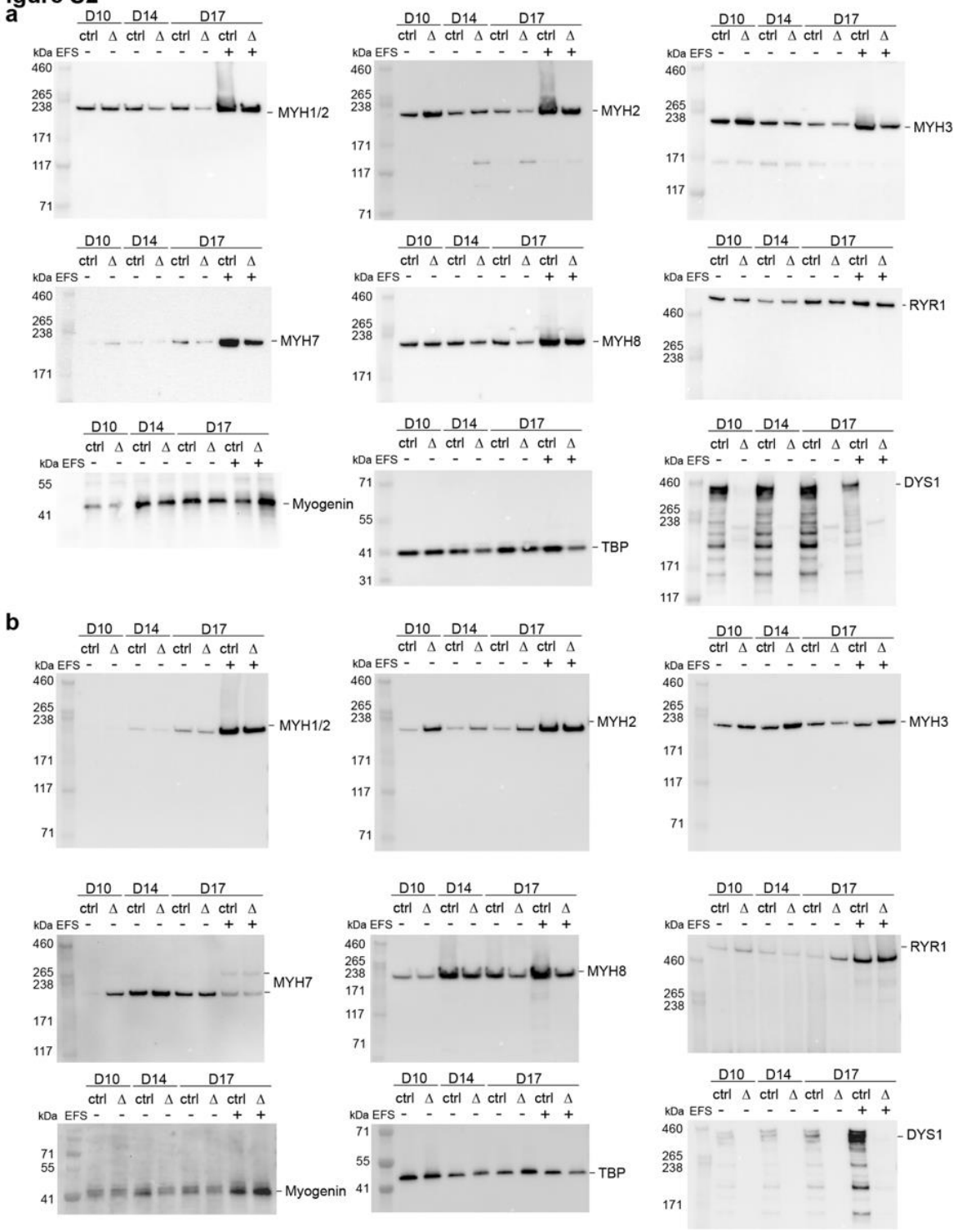

Figure S2. Western blot analysis of hiPSC-skeletal myotubes differentiated by the modified replating method in the absence or presence of EFS stimulation. (A-B) Western blotting using antibodies for differentiation and maturation-related markers. (A) DMDΔ44 clone (B) 409B2 clone. Related Figure 1 and 2.

Figure S3

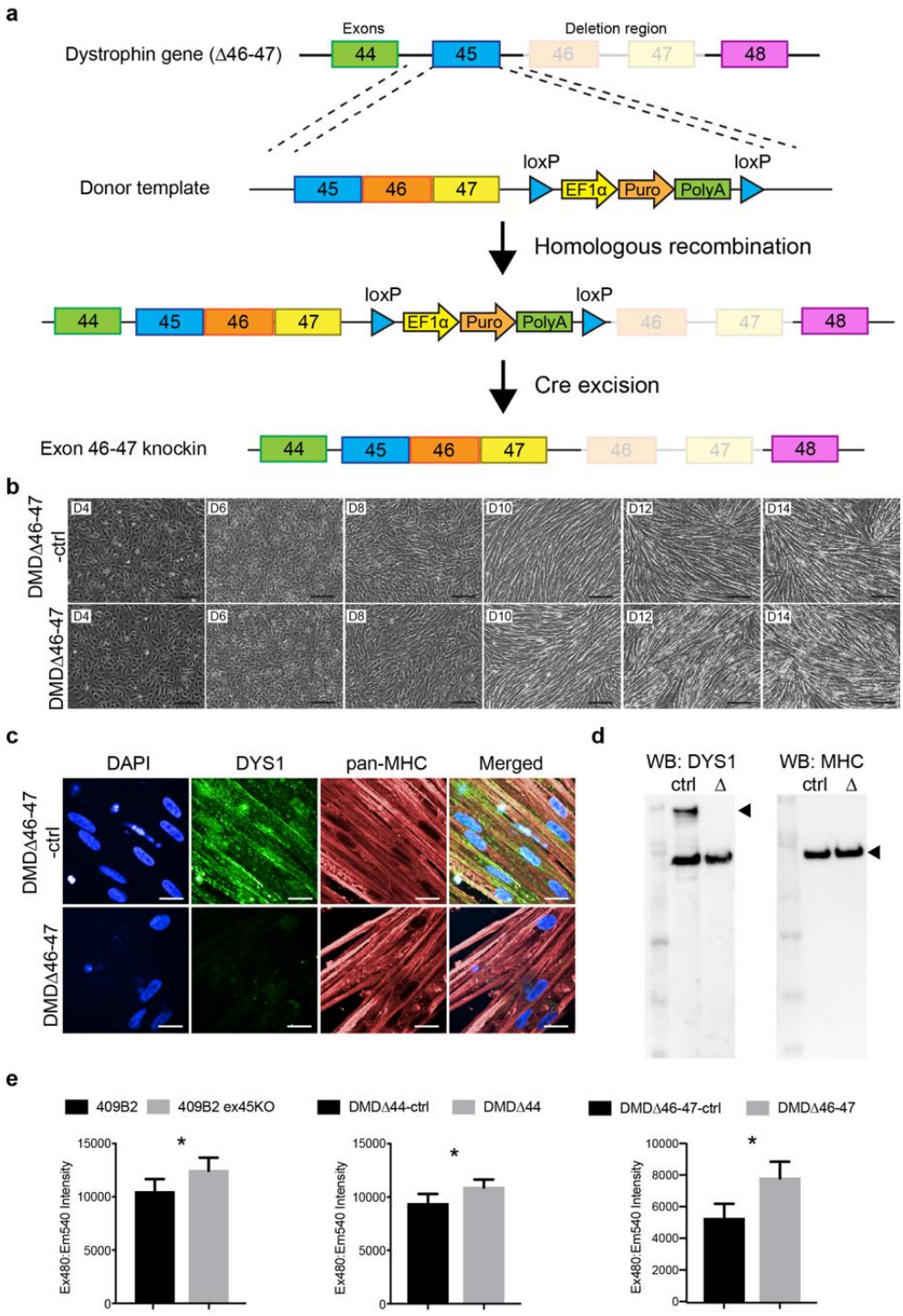

Figure S3. An isogenic control iPSC line of DMD-Δ 46–47 generated using a CRISPR/Cas9 knock-in. (A) A schematic diagram of CRISPR/Cas9-mediated exon 46–47 knock-in using DMD-Δ 46–47 iPSCs. (B) Bright-field images of time-course myogenic differentiation of DMD-Δ46-47-CKI and DMD-Δ 46–47 lines using the modified replating method. Scale bar = 200 μm. (C) Day 14 immunocytochemical analysis of pan-MHC and DYS1 in differentiated DMD-Δ46-47-CKI and DMD-Δ 46–47 myotubes using the modified replating method. Scale bar = 20 μm. (D) Day 14 western blot analysis of differentiated DMD-Δ46-47-CKI and DMD-Δ 46–47 myotubes using the modified replating method. Arrowheads indicate each band corresponding to full-length dystrophin and MHC. (E) The Ca^{2+} mobilization assay was conducted using an FDSS/μcell system. Quantitative analyses of differences of maximum and minimum Ca^{2+} peaks using 409B2, DMD-Δ44, and DMD-Δ 46–47 lines. Data represent the mean ± SD and were analyzed with an unpaired *t*-test from three biological replicates. * indicates $P < 0.05$. Related to STAR Methods.

Figure S4

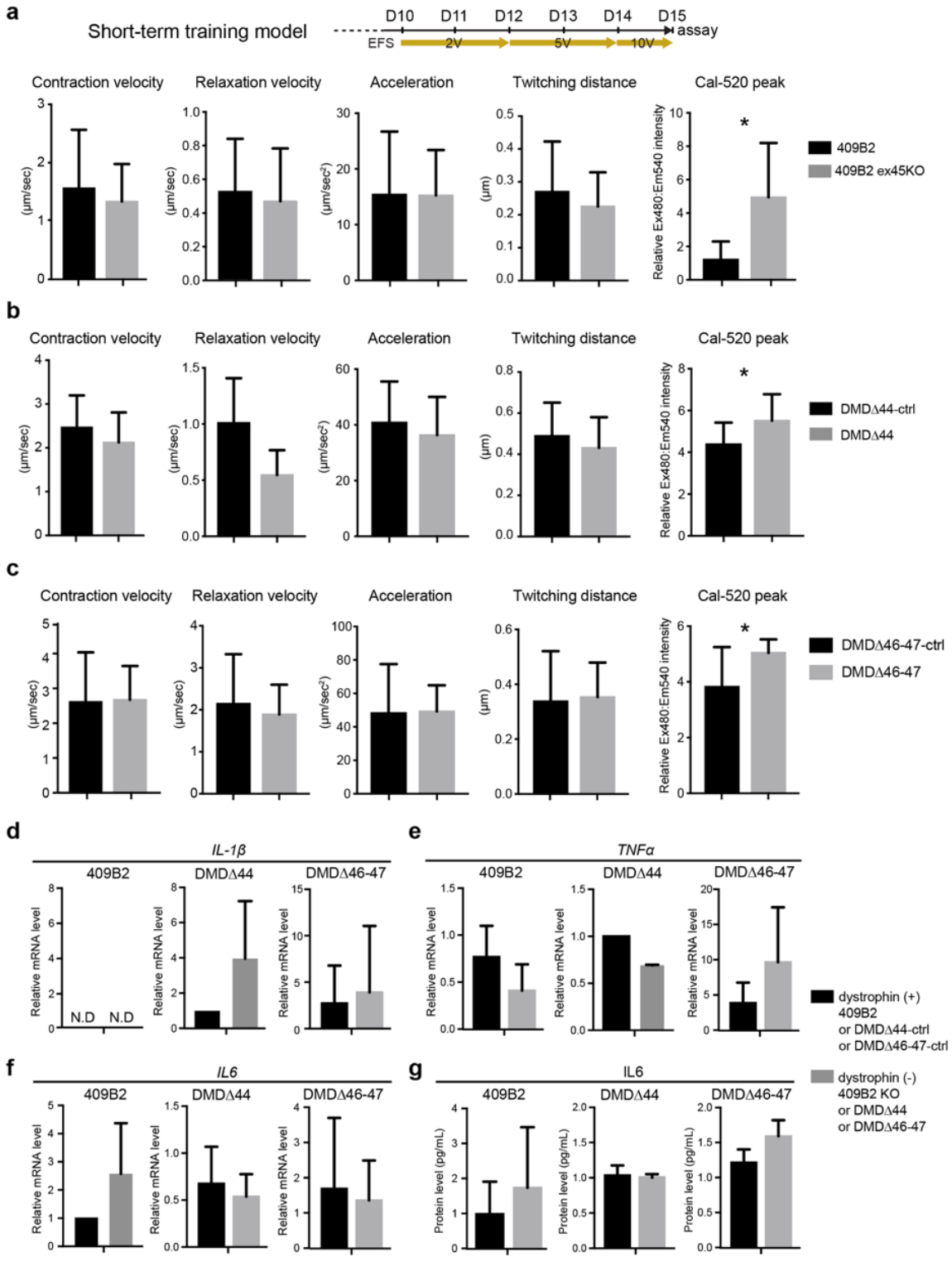

Figure S4. Comparable muscle performance observed in dystrophic myotubes at day 15 in the short-term EFS training model using three donor-derived iPSCs. (A-C) Functional analyses and Ca^{2+} peak assay in the short-term training model of differentiated and matured myotubes from three donor-derived iPSCs on day 15 using the SI8000 system. A: 409B2, B: DMDΔ44, C: DMDΔ46-47. (D–F) RT-qPCR analyses in the short-term training model of inflammation-related response-related genes on day 15. D: IL-1β, E: TNFα, F: IL6. (G) ELISA of IL6 protein levels in conditioned media harvested on day 15 from the short-term training model. Data represent the mean ± SD and were analyzed with an unpaired *t*-test from at least three biological replicates. * indicates $P < 0.05$. N.D = non-detectable. Related to Figure 3.

Figure S5

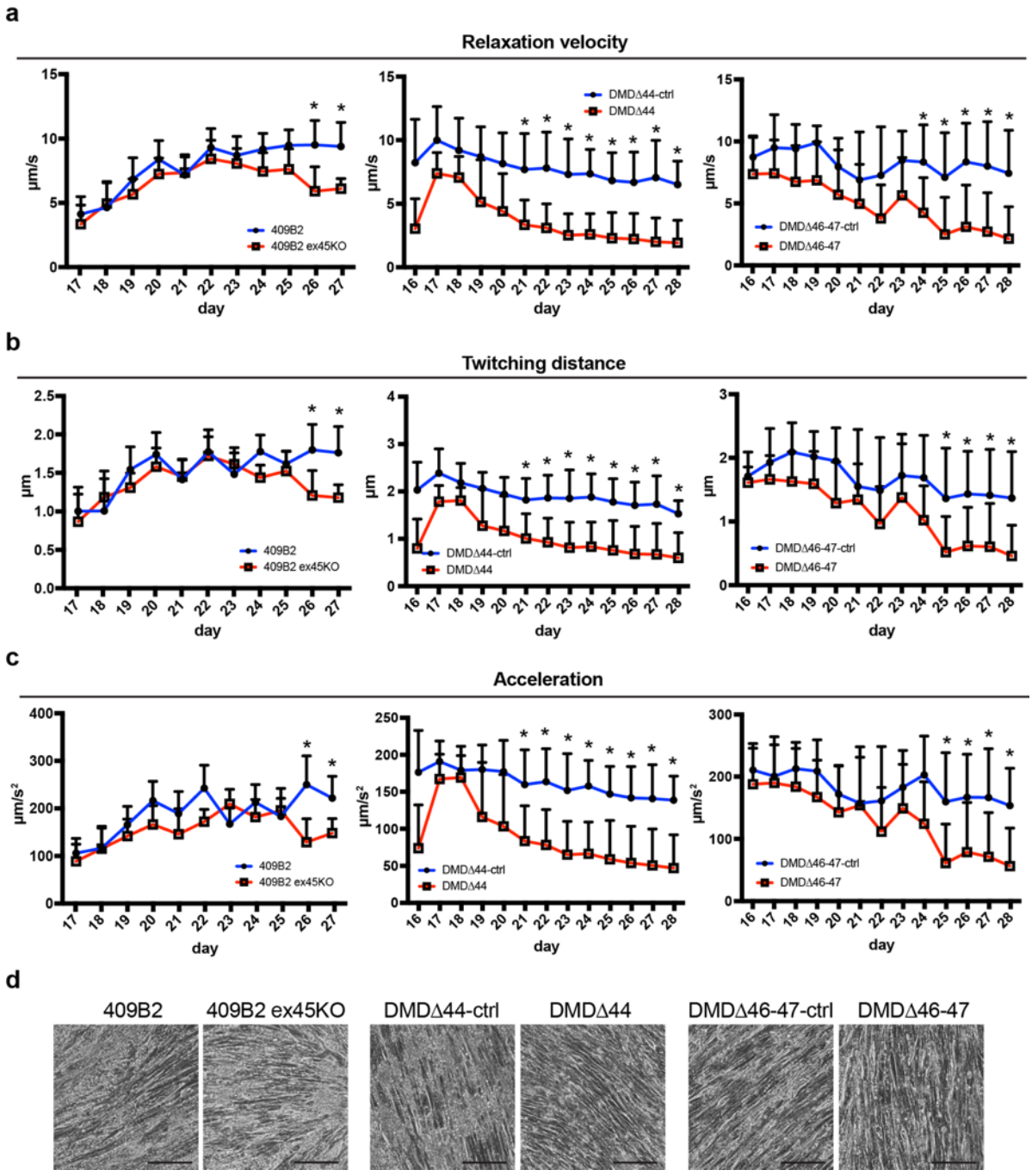

Figure S5. A gradual decline in muscle performance recapitulating the muscle fatigue-like symptoms of DMD was observed in dystrophic cells in the long-term EFS training model using three donor-derived iPSCs. (A–C) Quantitative time-course analyses of relaxation velocity, twitching distance, and acceleration using an SI8000 motion imaging system. A: 409B2, B: DMD-Δ44, C: DMD-Δ46-47. Data represent the mean ± SD and were analyzed with an unpaired *t*-test from at least three biological replicates. * indicates $P < 0.05$. (D) Bright-field images indicate that muscle fatigue-like symptoms did not accompany cellular damage or cell death in the long-term training model at day 28. Scale bar = 400 μm. Related to Figure 4.

Figure S6

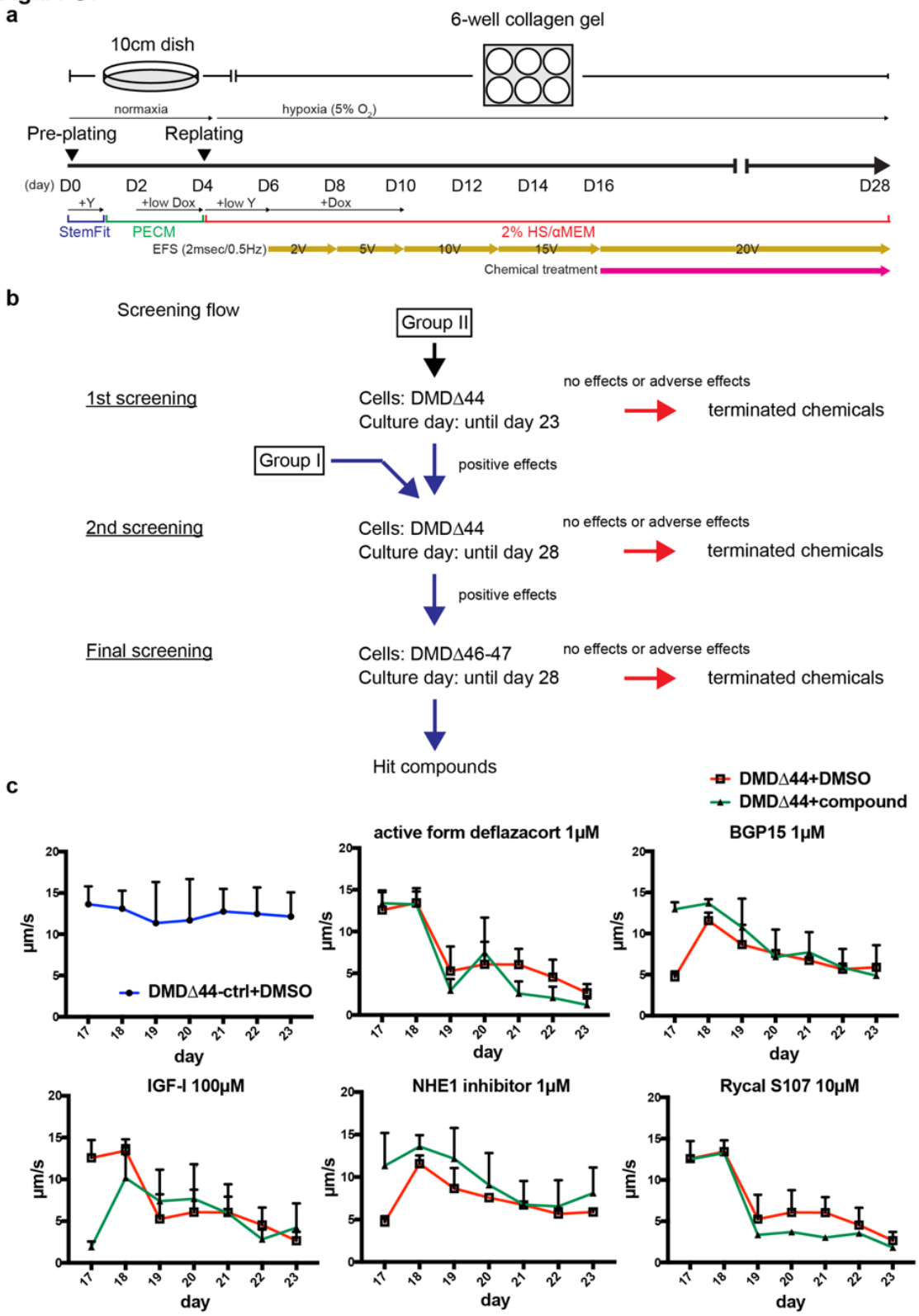

Figure S6. Small-scale screening in the long-term EFS training model. (A) A schematic diagram of each compound's administration in the long-term training model. (B) A schematic diagram of the screening strategy using two DMD patient-specific iPSCs, DMDΔ44 and DMDΔ 46–47. (C) Representative data from the first screening showing no or negative effects upon the administration of compounds. Data represent the mean ± SD and were analyzed with an unpaired *t*-test from at least three biological replicates. Related to Figure 5.

Figure S7

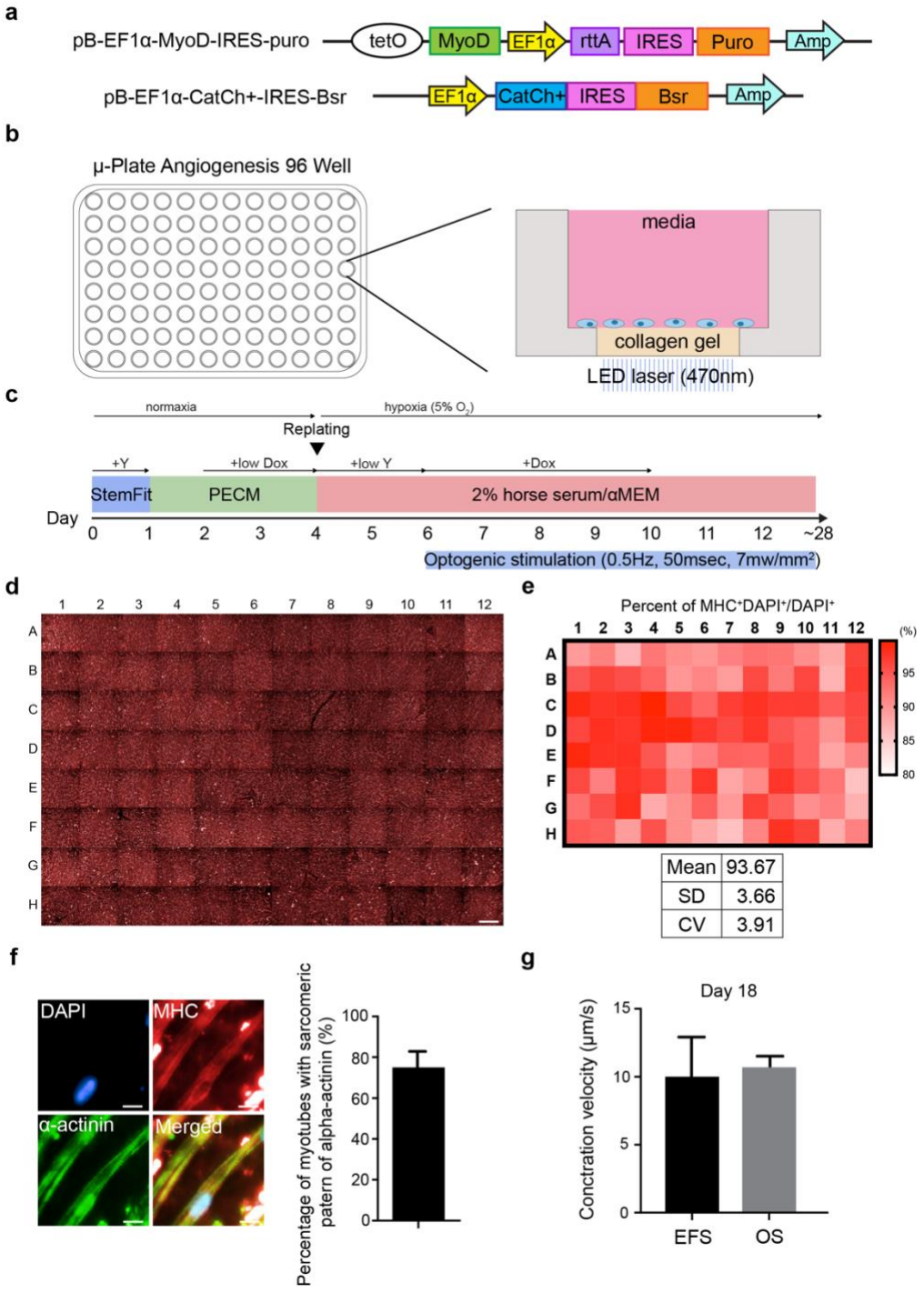

Figure S7. A 96-well plate screening model using optogenetic technology. (A) The plasmids map used to establish iPSC clones stably expressing dox-inducible MyoD and CatCh+, a channelrhodopsin-2 variant. (B) An image of a μ-plate Angiogenesis 96 well plate and collagen gel preparation in the bottom layer of the plate. Optogenetics stimulation (OS) training was applied to cells using a blue (470 nm) LED laser from the bottom of the plate, leading to the cell membrane depolarization. (C) An OS protocol. (D) Representative immunofluorescent staining of pan-MHC at day 28 in the long-term training model under OS (scale bar = 200μm) and (E) statistical analysis to calculate the coefficient value. (F) Fusion index analysis of DMDΔ44 myotubes at day 18 under OS. (G) Immunofluorescent staining of pan-MHC and α-actinin on differentiated iPSC-myotubes at day 18 under OS. Scale bar = 20 μm. (H) Contractile performance of DMDΔ44 myotubes at day 18 under EFS and OS. Data represent the mean ± SD from five biological replicates. Related to Figure 6.